Evolution of a localized electron spin in a nuclear spin environment

Sigurdur I. Erlingsson* and Yuli V. Nazarov
Delft University of Technology, Department of NanoScience, Lorentzweg 1, 2628 CJ Delft, The Netherlands
(Dated: February 2, 2008)

Motivated by recent interest in the role of the hyperfine interaction in quantum dots we study the dynamics of a localized electron spin coupled to many nuclei. An important feature of the model is that the coupling to an individual nuclear spin depends on its position in the quantum dot. We introduce a semi-classical description of the system valid in the limit of a large number of nuclei and analyze the resulting classical dynamics. Contrary to a natural assumption, the correlation functions of electron spin with an arbitrary initial condition show no decay in time. Rather, they exhibit complicated undamped oscillations. This may be attributed to the fact that the system has many integrals of motion and is close to an integrable one. The ensemble averaged correlation functions do exhibit a slow decay ($\sim 1/\ln(t)$) for $t \to \infty$.

PACS numbers: 73.21.La,85.35.Be,72.25.Rb

I. INTRODUCTION

The coherent manipulation of localized spins in solid state systems is currently a very active field research[1]. One of the most ambitious goals in this field of research is developing a quantum bit, or qubit. Such qubits would form the basic building blocks of quantum computers[2,3,4,5]. The strength of the qubit coupling to the environment should be sufficiently well controlled so that the residual environmental interactions are below a threshold set by the operating speed of the device[6,7,8].

Since the first proposal in Ref. 4, the qubit candidate based on localized electron spins in quantum dots has been the subject of many theoretical and experimental studies. There have already been quite a few studies of the relaxation time of electron spins in GaAs quantum dots. The role of various spin-orbit related mechanisms has been considered for spin-flip transitions between singlet and triplets[9] and Zeeman split doublets[10]. The hyperfine mediated spin-flip rates were investigated for singlet-triplet[11] and doublet[12] transitions. A novel spin-flip mechanism due to interface motion has also been investigated[13] and Coulomb blockade effects in the nuclear spin relaxation time were looked at in Ref. 14. For GaAs quantum dots measurements of spin relaxation times, or T_1, between singlet-triplet states[15,16] and doublet[17] states have been done. The measurements give $T_1 \approx 200\,\mu$s (singlet-triplet) and $T_1 > 50\,\mu$s (doublet). For the doublet measurements only a lower bound for the relaxation time is obtained[17], so comparison to various theoretical calculations remains difficult.

The operation of a qubit requires a coherent superposition of states that persists during the time of the qubit operation. Several papers have addressed the question of the decoherence time of electron spin in GaAs quantum dots. The decoherence of a single electron spin may be caused by inhomogeneous hyperfine interaction[18,19] but when an ensemble of electron spins is considered the timescale of decoherence is determined by the fluctuations in the total field which acts on the electron spin due to the nuclei[20,21]. The role of fluctuations in the nuclear spin system, socalled spectral diffusion, on the electron spin decoherence has also been studied[22,23].

In Ref. 18 the characteristic timescale for the decay of a specific correlation function was associated with the decoherence time of the electron spin. The decohence in this case was attributed to the spatially dependent hyperfine coupling constant which caused small frequency changes through flip-flop processes involving spatially separated nuclei. A different approach was used in Ref. 20 which relied on representing the nuclear spin system as an effective nuclear magnetic field that couples to the electron spin in the quantum dot. Merkulov *et al.* discussed some basic features of this semi-classical approach but the calculations were done for ensemble averaged quantities[20].

In the present work we combine the approaches mentioned and extend the semiclassical effective-field method[12] to include the effects of the spatially varying hyperfine coupling constant. Due to the large difference of timescales for the electron and nuclear spin systems we are able to solve the problem in two steps. In the first step we establish that the nuclear system can be treated as an adiabatic effective nuclear magnetic field acting on the electron. The latter step involves the back action of the electron spin which will determine the evolution of the nuclear spins. The fact that the single electron spin is coupled to a large number of nuclei in the quantum dot, N, but each nucleus is only coupled to the single electron spin hints at an asymmetry in the behavior of the electron and nuclear spins. The electron precesses in an effective nuclear magnetic field which is due to the whole nuclear spin system. This field is $\propto \sqrt{N}$ times larger than the corresponding hyperfine field due to the single electron spin in which the nuclear spins precess. Thus the dynamics of the electron are much faster than the dynamics of the nuclei. Also, the large number of nuclei involved makes it possible to treat the nuclear system in a semi-classical way[12,20,24]. We do not include the dipole-dipole interaction of the nuclei, since the effects of such interaction can only become noticeable at very long timescale ($t_{\rm dip} \simeq 10^{-3}$sec, for GaAs quantum dots[20,25]).

The resulting dynamics are represented by a set of

equations of motion for several subsystems of nuclear spins. Each subsystem is characterized by the same value of coupling to the electron spin. The dynamical equations are non-linear and comprise many degrees of freedom. From this, one generally expects chaotic and ergodic dynamics, so that the memory about initial conditions is lost at a certain time scale. This would result in the decay of correlation functions at this time scale and was an initial motivation of this research. However, we prove that the actual dynamics is not chaotic. The calculated correlation functions show complex, yet regular, oscillations that persist for long timescale without discernible decay. We explain this by conjecturing that the system has many integrals of motion so it is close to exactly integrable one.

If we average the dynamics over all possible initial conditions, the averaged correlation function does show decay in time. For large times, it is inversely proportional to logarithm of time.

The remaining text of the paper is organized as follows. In Sec. II the hyperfine interaction in a quantum dot is presented and its semi-classical representation discussed. The adiabatic approximation for the electron spin dynamics is discussed in Sec. III and some analytic properties of the dynamical equations are presented in Sec. IV. The correlation functions used to characterize the dynamics are introduced in Sec. V and finally the results of the numerical calculations are discussed in Sec. VI.

II. HYPERFINE INTERACTION IN QUANTUM DOTS AND ITS SEMI-CLASSICAL REPRESENTATION

The Hamiltonian describing the hyperfine coupling between conduction band electrons and the lattice nuclei in GaAs is of the well known form of the contact potential

$$H_{\rm HF} = A\hat{\boldsymbol{S}} \cdot \sum_k \hat{\boldsymbol{I}}_k \delta(\boldsymbol{r} - \boldsymbol{R}_k), \tag{1}$$

where A is the hyperfine constant, $\hat{\boldsymbol{S}}$ ($\hat{\boldsymbol{I}}_k$) and $\boldsymbol{r}$ ($\boldsymbol{R}_k$) are respectively the spin and position of the electron (kth nuclei). In the GaAs conduction band (which is mainly composed of s-orbitals), the dipole-dipole part of the hyperfine interaction vanishes[26]. In this paper the focus will be on electrons localized in a quantum dot, and the hyperfine interaction in such systems. The quantum dots considered here are quite general, but we introduce some restrictions to simplify the model. First of all it is assumed that the number of electrons is fixed, preferably to one. From the experimental point of view this assumptions is quite reasonable since having only a single electron in the dot has already been demonstrated experimentally[27,28]. The second assumption is that the orbital level splitting is much larger than the hyperfine energy. In this case the hyperfine Hamiltonian can be projected to the lowest orbital level since contributions from higher orbitals are strongly suppressed due to the large orbital energy separation. If the ground state orbital $\psi(\boldsymbol{r})$ of the quantum dot is known, then an effective spin Hamiltonian can be written as

$$H_{\rm s} = g\mu_B \boldsymbol{B} \cdot \hat{\boldsymbol{S}} + \gamma_{\rm GaAs} \sum_k \boldsymbol{B} \cdot \hat{\boldsymbol{I}}_k + \sum_k A|\psi(\boldsymbol{R}_k)|^2 \hat{\boldsymbol{S}} \cdot \hat{\boldsymbol{I}}_k \tag{2}$$

where g is the g-factor, μ_B is the Bohr magneton, $\gamma_{\rm GaAs}$ is the gyromagnetic ratio of the effective nuclear species and $\boldsymbol{B}$ is the external applied field.

In a typical quantum dot a single electron spin may be coupled to $10^4 - 10^6$ nuclear spins. When the electrons interacts with so many nuclei it is possible to interpret the combined effect of the nuclei as an effective magnetic field. Before proceeding further it is convenient to introduce a different way of writing the hyperfine interaction in the last term in Eq. (2). The wave function of the ground state orbital has some characteristic spatial extent which is determined by the confining potential. Without loss of generality it may be assumed that the lateral (with respect to the underlying 2DEG) and transverse confining lengths are ℓ and z_0 respectively. Defining the volume of the quantum dot as $V_{\rm QD} = \pi z_0 \ell^2$, a dimensionless function is introduced:

$$f(\boldsymbol{R}_k) = V_{\rm QD}|\psi(\boldsymbol{R}_k)|^2. \tag{3}$$

Furthermore, denoting the maximum value of f with $f_{\rm Max}$ we introduce a dimensionless coupling constant

$$g_k = g(\boldsymbol{R}_k) = \frac{f(\boldsymbol{R}_k)}{f_{\rm Max}} \in (0,1). \tag{4}$$

The hyperfine coupling constant may be expressed in terms of the concentration, C_n, of nuclei with spin I and a characteristic energy E_n through the relation $A = E_n/C_n I$. The energy E_n is the maximum Zeeman splitting possible due to a fully polarized nuclear system, its value being $E_n \approx 0.135\,\text{meV}$ in GaAs[29,30]. The hyperfine interaction term can thus be written as

$$H_{\rm HF} = \hat{\boldsymbol{S}} \cdot \hat{\boldsymbol{K}}, \tag{5}$$

where we have introduced the operator for the effective nuclear magnetic field

$$\hat{\boldsymbol{K}} \;=\; \gamma \sum_k g_k \hat{\boldsymbol{I}}_k, \tag{6}$$

and the characteristic hyperfine induced nuclear spin precession frequency

$$\gamma = \frac{E_n f_{\rm Max}}{NI}. \tag{7}$$

As was shown in Ref. 12 it is possible to replace the operator in Eq. (6) with a effective nuclear magnetic field $\boldsymbol{K}$. Its initial value is random since it is determined by unknown details of the nuclear system. Assuming that

the nuclear spin system temperature $k_BT \gg \gamma$, all nuclear states are equally likely to be occupied. Initially the nuclei are nominally decoupled from each other and the distribution of $\boldsymbol{K}$ is to a good approximation represented by a Gaussian[12,20]

$$P(\boldsymbol{K}) = \left(\frac{3}{2\pi\gamma^2 N\overline{I^2}}\right)^{3/2} \exp\left(-\frac{3\boldsymbol{K}^2}{2\gamma^2 N\overline{I^2}}\right), \quad (8)$$

where $\overline{I^2} = I(I+1)N^{-1}\sum_k g_k^2$.

In the above discussion the dynamics of the nuclear spin system was disregarded. Before we include its dynamics it is instructive to first derive *exact* operator equations of motion, and then apply the semi classical approximation to those equations. The dynamics of the combined electron and nuclear spin systems are determined by the Heisenberg equation of motion

$$\frac{d}{dt}\hat{\boldsymbol{S}} = \hat{\boldsymbol{K}} \times \hat{\boldsymbol{S}} + g\mu_B \boldsymbol{B} \times \hat{\boldsymbol{S}}, \quad (9)$$

$$\frac{d}{dt}\hat{\boldsymbol{I}}_k = \gamma g_k \hat{\boldsymbol{S}} \times \hat{\boldsymbol{I}}_k + \gamma_{\mathrm{GaAs}} \boldsymbol{B} \times \hat{\boldsymbol{I}}_k. \quad (10)$$

Multiplying Eq. (10) with g_k and summing over k gives the equation of motion for $\hat{\boldsymbol{K}}$

$$\frac{d}{dt}\hat{\boldsymbol{K}} = \gamma \hat{\boldsymbol{S}} \times \left(\sum_k g_k^2 \hat{\boldsymbol{I}}_k\right) + \gamma_{\mathrm{GaAs}} \boldsymbol{B} \times \hat{\boldsymbol{K}}. \quad (11)$$

In contrast to the simple dynamics of Eq. 9, the equation of motion for $\hat{\boldsymbol{K}}$ is quite complicated. The reason for the asymmetry is the position dependent coupling g_k. The quantity in the brackets on the rhs of Eq. (11) cannot be expressed in terms of $\hat{\boldsymbol{K}}$. Only in the simple case of constant g_k it is possible to write a closed equation of motion for $\hat{\boldsymbol{K}}$ and $\hat{\boldsymbol{S}}$.[21] Without actually solving Eqs. (9) and (11) it is still possible to extract general features of the dynamics. For zero external magnetic field, the electron spin will precess with frequency $\propto E_n N^{-1/2}$ (which is the magnitude of the effective nuclear magnetic field) and the nuclear system precesses with frequency $\propto E_n N^{-1}$. Thus, for $N \gg 1$, the electron spin effectively sees a stationary nuclear system and in turn the nuclear system sees a time averaged electron spin.

To incorporate (i) the separation of timescales and (ii) the inhomogeneous coupling we introduce a scheme that separates the nuclear system into N_b subsystems, each being characterized by a fixed coupling g_b. The effective nuclear magnetic field of a given subsystem is

$$\hat{\boldsymbol{K}}_b = \gamma g_b \sum_{k\in b} \hat{\boldsymbol{I}}_k \quad (12)$$

where the notation $k \in b$ is shorthand for all nuclei whose coupling is $g_k \in [g_b - \delta g/2, g_b + \delta g/2]$, with $\delta g = 1/N_b$ being the coupling constant increment. As long as $N_b \ll N$ each subsystem can be replaced by a classical variable $\hat{\boldsymbol{K}}_b \to \boldsymbol{K}_b$, which represents the effective nuclear field due to that particular nuclear spin subsystem.

Using the same procedure as was used in deriving Eq. (11) we arrive at a equation of motion for $\hat{\boldsymbol{K}}_b$ and applying the semi-classical approximation results in

$$\frac{d\boldsymbol{K}_b}{dt} = \gamma g_b \langle \boldsymbol{S}\rangle \times \boldsymbol{K}_b + \gamma_{\mathrm{GaAs}} \boldsymbol{B} \times \boldsymbol{K}_b, \quad (13)$$

where $\langle \boldsymbol{S}\rangle$ is an appropriate time averaged electron spin. As will be discussed in the next section, this average electron spin may be written as a function of the total effective nuclear field

$$\boldsymbol{K} = \sum_b \boldsymbol{K}_b. \quad (14)$$

The initial condition for each nuclear spin subsystem is randomly chosen from a Gaussian distribution whose variance is (see Appendix A)

$$\langle \boldsymbol{K}_b^2\rangle = \gamma^2 N I(I+1) g_b \delta g. \quad (15)$$

The set of differential equations in Eq. (13), with the associated random initial conditions constitute a set of autonomous differential equations.

Separating the nuclear system into subsystem with a constant g_b is an approximation to the continuous coupling g_k. As the number of subsystems increases g_b will more closely represent g_k. However, for the semi-classical approximation to be valid each subsystem must contain many nuclear spins. Thus, increasing N_b should better reproduce the actual system, as long as $N_b \ll N$.

III. ADIABATIC APPROXIMATION FOR THE ELECTRON SPIN

As we have shown in the previous section, the nuclear spin system may be treated as a slowly varying effective nuclear magnetic field acting on the electron spin. Letting $\boldsymbol{H}(t)$ represents any slowly varying magnetic field (fulfilling the usual adiabatic conditions) acting on a single electron spin, leads to the Hamiltonian

$$H_e(t) = \hat{\boldsymbol{S}} \cdot \boldsymbol{H}(t). \quad (16)$$

It is convenient to introduce the instantaneous eigenfunctions of the Hamiltonian, which are solutions of

$$H_e(t)|\boldsymbol{n}(t);\pm\rangle = E_\pm(t)|\boldsymbol{n}(t);\pm\rangle. \quad (17)$$

The eigenstates are labeled by $\boldsymbol{n}(t)$ to indicate that these eigenstates are either pointing 'up' (+) or 'down' (-) along the total magnetic field, whose direction is determined by the unit vector

$$\boldsymbol{n}(t) = \frac{\boldsymbol{H}(t)}{|\boldsymbol{H}(t)|}. \quad (18)$$

For a spin 1/2 in an external field, the eigenenergies are $E_\pm(t) = \pm\frac{1}{2}|\boldsymbol{H}(t)|$, and the corresponding eigenstates are written in the basis of the $\hat{S}_z$ eigenvectors

$$\begin{pmatrix} |\boldsymbol{n}(t);+\rangle \\ |\boldsymbol{n}(t);-\rangle \end{pmatrix} = \frac{1}{\sqrt{1+|a(t)|^2}} \begin{pmatrix} |\uparrow\rangle + a(t)|\downarrow\rangle \\ |\downarrow\rangle - a^*(t)|\uparrow\rangle \end{pmatrix}. \quad (19)$$

The time dependent mixing of spin components is given by

$$a(t) = \frac{|\boldsymbol{H}(t)| - H_z(t)}{H_x(t) - iH_y(t)}. \tag{20}$$

The wave function may be expanded in basis of instantaneous eigenstates

$$|\psi(t)\rangle = \sum_{\sigma=\pm} c_\sigma(t)|\boldsymbol{n}(t);\sigma\rangle \tag{21}$$

where the expansion coefficients are

$$c_\pm(t) = c_\pm(t_0)e^{\left(i\gamma_\pm(t) - \frac{i}{\hbar}\int_{t_0}^{t} d\tau E_\pm(\tau)\right)}. \tag{22}$$

The additional phase factor appearing in the previous equation is the usual adiabatic phase[31]

$$\gamma_\pm(t) = i\int_{t_0}^{t} d\tau \langle \boldsymbol{n}(\tau);\pm|d/d\tau|\boldsymbol{n}(\tau);\pm\rangle. \tag{23}$$

Integrating by parts the rhs of the last equation and using the orthogonality of the instantaneous eigenstates, it can be shown that the phase $\gamma_\pm$ is a real number. Also, for a doublet $\gamma \equiv \gamma_+ = -\gamma_-$.

Using the wave function in Eq. (21), the average electron spin is

$$\begin{aligned}\langle \hat{\boldsymbol{S}}(t)\rangle &\equiv \langle\psi(t)|\hat{\boldsymbol{S}}|\psi(t)\rangle \\ &= \sum_{\sigma=\pm} |c_\sigma(t_0)|^2 \langle \boldsymbol{n}(t);\sigma|\hat{\boldsymbol{S}}|\boldsymbol{n}(t);\sigma\rangle \\ &+ 2\Re\left\{c_+^*(t_0)c_-(t_0)e^{\left(-2i\gamma(t) - \frac{i}{\hbar}\int_{t_0}^{t} d\tau|\boldsymbol{H}(\tau)|\right)}\right\}\end{aligned} \tag{24}$$

The latter term in Eq. (24) oscillates with frequency $|\boldsymbol{H}(t)|/h \gg E_n N^{-1}/h$, so its average is zero on the timescales of the nuclear system. The average value of the electron spin entering Eq. (13) is

$$\begin{aligned}\langle \boldsymbol{S}\rangle &= \sum_{\sigma=\pm} |c_\sigma(t_0)|^2 \langle \boldsymbol{n}(t);\sigma|\hat{\boldsymbol{S}}|\boldsymbol{n}(t);\sigma\rangle \\ &= \frac{1}{2}\cos(\theta_0)\frac{\boldsymbol{H}(t)}{|\boldsymbol{H}(t)|},\end{aligned} \tag{25}$$

where θ_0 is the angle between the initial electron spin and $\boldsymbol{n}(0)$, see Fig. 1. The orientation between $\boldsymbol{S}$ and $\boldsymbol{n}(0)$ changes the precession of all $\boldsymbol{K}_b$'s by a multiplicative factor $\cos\theta_0$. This overall factor has no effect on the dynamics and we subsequently put it to unity. Physically, one might think of a dissipation mechanism that would initially align the electron spin and $\boldsymbol{H}$ to each other, although the mechanism itself is not critical for the following discussion.

From the semi-classical version of Eq. (9), the slowly varying magnetic field is $\boldsymbol{H}(t) = \boldsymbol{B} + \boldsymbol{K}(t)$ which results in an equation for $\langle \boldsymbol{S}\rangle$ that depends only on $\boldsymbol{K}$ and $\boldsymbol{B}$. Also, since we assume that the quantum dot is initially in the ground state orbital and that the orbital energy separation is much larger than the hyperfine energy, there are no 'Rabi oscillations' to higher orbitals.

IV. SOME ANALYTIC PROPERTIES

The rest of the paper will only consider the case of small magnetic field $g\mu_B\boldsymbol{B} \ll \boldsymbol{K}$, which is the regime where the dynamics are most interesting. In the opposite situation the magnetic field strongly constraints all dynamics. The average electron spin, for $\boldsymbol{B} = 0$ is

$$\langle \boldsymbol{S}\rangle = -\frac{1}{2}\frac{\boldsymbol{K}}{|\boldsymbol{K}|} \tag{26}$$

and the resulting equation of motions for the nuclear spin subsystems are

$$\frac{d}{dt}\boldsymbol{K}_b = \tilde{\gamma} g_b \boldsymbol{K}\times\boldsymbol{K}_b, \tag{27}$$

where $\tilde{\gamma} = -\gamma/2|\boldsymbol{K}|$, since $|\boldsymbol{K}|$ is a constant of motion

$$\frac{d}{dt}|\boldsymbol{K}|^2 = 0, \tag{28}$$

and it equally changes the precession frequency of all the block $\boldsymbol{K}_b$. In addition to $|\boldsymbol{K}|$, more integrals of motion can be constructed from Eq. (27):

$$0 = \frac{d}{dt}|\boldsymbol{K}_b|^2 \tag{29}$$

$$0 = \frac{d}{dt}\boldsymbol{I} = \frac{d}{dt}\left(\sum_b \frac{\boldsymbol{K}_b}{g_b}\right) \tag{30}$$

$$0 = \frac{d}{dt}\left(\boldsymbol{I}\cdot\left(\sum_b \frac{\boldsymbol{K}_b}{g_b^2}\right)\right). \tag{31}$$

The integral of motion in Eq. (30), is actually the total spin $\boldsymbol{I}$ of the nuclear system[20]. The integrals of motion are expected to affect the dynamics, i.e. the system will be 'constrained' by them.

The solution for the electron dynamics is determined by the dynamics of the nuclear system, which is encapsulated in $\boldsymbol{K}(t)$. Although the dynamics are complicated there are some ways to characterize the motion of the nuclear system. For example, we can define the following quantity

$$\boldsymbol{K}(t;\zeta) = \sum_b \frac{1}{1+\gamma_b\zeta}\boldsymbol{K}_b(t) \tag{32}$$

which satisfies the following equation of motion

$$\frac{d}{dt}\boldsymbol{K}(t;\zeta) = \frac{\boldsymbol{K}(t;0)\times\boldsymbol{K}(t;\zeta)}{\zeta}. \tag{33}$$

It is possible to construct other similar equations, but in general no simple solution for them exist.

V. CORRELATION FUNCTIONS

A wide class of classical systems exhibits decaying correlation functions. This occurs in classically chaotic systems in which the motion is such that the memory about

initial conditions is lost at some typical timescale[32]. Most of sufficiently complicated classical systems are eventually chaotic. One might expect that the set of equations Eq. (13) should describe chaotic dynamics and decay of correlation functions. We will see later on that this is not the case.

A useful way to characterize the electron spin dynamics it is to introduce certain correlation functions. For an isolated quantum system these correlation function are expected to oscillate periodically, without any decay. Incorporating environmental effects usually shows up in modified behavior of the correlation functions. The expected behavior is that they should decay as a function of time. To investigate how the nuclear spin system acts as a spin bath (environment), we introduce the following correlation function

$$G(t) \;=\; \langle\uparrow|\hat{\boldsymbol{S}}(t)\cdot\hat{\boldsymbol{S}}|\uparrow\rangle, \tag{34}$$

where the time evolution of the operators is in the usual Heisenberg picture.

Since we are focusing on the slow dynamics it is useful to write these correlation functions for long timescales. In the adiabatic approximation the correlation functions may be written as

$$G(t) \;=\; \frac{1}{4}\frac{(1-|a(t)|^2)(1-|a(0)|^2)+4a(t)a^*(0)}{(1+|a(t)|^2)(1+|a(0)|^2)}, \tag{35}$$

where the a's are defined in Eq. (20). The most interesting regime corresponds to weak external magnetic fields. In this case there is no preferred direction and the dynamics show the richest behavior. In that limit the correlation functions take the simplified form

$$G(t) = \frac{\boldsymbol{K}(t)\cdot\boldsymbol{K}(0)}{4K(t)K(0)} \tag{36}$$

From these equations it is evident that the electron spin correlation function is determined by the nuclear system variables for times $t \gg \hbar\sqrt{N}/E_n$.

When dealing with many identical systems in which the electron can be prepared in a given initial state but the effective nuclear magnetic fields differ in the initial values, ensemble averaged correlation function must be considered. No information is available about the state of the effective nuclear magnetic field, except that their initial vales are Gaussian distributed. In this case the correlation function in Eq. (35) should be averaged over the appropriate distributions

$$\langle G(t)\rangle = \int\prod_b d\boldsymbol{K}_{b,0}P(\{\boldsymbol{K}_{b,0}\})G(t;\{\boldsymbol{K}_{b,0}\}), \tag{37}$$

where $\boldsymbol{K}_{b,0} = \boldsymbol{K}_b(0)$ and P is the Gaussian distribution of the initial values. Note that the correlation functions appearing in Eq. (36) are also functions of the set of initial conditions $\{\boldsymbol{K}_b(0)\}$.

VI. RESULTS

The correlation functions in Eqs. (36) and (37) are in general not exactly solvable so numerical simulations have to be used. In order to calculate them time series for $\boldsymbol{K}_b(t)$ need to be calculated. These are obtained by numerically integrating the differential equations in Eq. (27). We focus on the case of no external magnetic field. In GaAs $\gamma \approx 10^{-7}\,\mathrm{meV}\approx 10^5\,\mathrm{Hz}$ for quantum dots containing $N \approx 10^6$ nuclei. The differential equations are solved by integrating numerically Eq. (27) using the 4th order Runge Kutta method. The $K_b(t)$'s are then used to calculate $a(t)$ that enter Eq. (35).

For the ensemble averaged correlation functions many sets of time series $\{\boldsymbol{K}_b(t)\}$ are calculated, each corresponding to different random initial condition chosen from a Gaussian distribution. The results for the ensemble averaged correlation function in Eq. (37) are presented in Fig. 2. Each curve is the result of calculations for different number of subsystems $N_b = 4, 8, \ldots, 512$. As is to be expected, the correlation functions decay in time but a saturation value is reached for sufficiently long times, which is determined by $t_{\rm sat} \propto \gamma^{-1}N_b$. This saturation is an artifact of the discretization, i.e. it introduces a time above which the calculated correlation function no longer represents the true correlation function. For the calculated correlation function to have a meaningful limit, the saturation value should approach zero as N_b increases and the saturation time should go to infinity. The inset in Fig. 2 plots the saturation values of $\langle G(t)\rangle$. It is evident that the saturation values tend to zero for larger N_b. The decay fits an inverse logarithm $\alpha/\ln(\beta N_b)$ quite well. This indicates that there is a well defined $N_b \to \infty$ correlation function which has an inverse logarithmic decay $\propto 1/\ln t$ as $t \to \infty$. The origin of the logarithmic decay is not fully understood (and thus the theoretical values of α and β) but it might be related to the total spin $|\boldsymbol{I}|^2 \propto \ln t_{\rm sat}$ (see Appendix A). The correlation function is normalized and its value might be dominated by $1/|\boldsymbol{I}|^2$ for $t > t_{\rm sat}$.

The correlation functions for a single system, i.e. without taking the ensemble average, yield quite different results. The calculations are performed for $N_b = 8, 32, 128$ and 256. For each number of subsystems N_b the calculations were repeated for various random initial conditions, but no averaging is performed. The results of the calculations for $G(t)$ are presented in Figs. 3-6 (note different range on the horizontal, or t-axis). The common feature of all the curves, for all values of N_b, is that they do not decay with time. This behavior persists to even longer times, not shown here. Even though more complicated behavior is observed for large N_b, the characteristic frequencies of the correlation function oscillations do not show any obvious dependence on the number of subsystems.

It is instructive to look at the power spectrum of $G(t)$, where the oscillating behavior of the correlation functions becomes more apparent. The power spectrum (or

the squared Fast Fourier Transform) of $G(t)$ is shown for the 1st and 6th curves (counted from the bottom one) for $N_b = 32$ (see Fig. 4), in Figs. 7 and 8 respectively. The sharp, isolated peaks in the spectra illustrate well the multi-periodic oscillations observed in $G(t)$. This behavior is still present in the power spectra for $N_b = 256$. Figs. 9-11, corresponding to respectively the 2nd, 4th and 6th curves in Fig. 6, show that even for such a complicated system (256 coupled, non-linear differential equations) the correlation functions still show sharp, isolated peaks corresponding to well defined oscillation periods and additional many smaller, closely spaced peaks.

The power spectrum is the Fourier spectrum of the *time averaged* correlation functions, which are completely different from the power spectra expected for the ensemble averaged correlation functions shown in Fig. (2). This implies that the time average and the ensemble average are not equivalent, i.e. the system in question is not ergodic. The simplest way to think about this is to consider the integrals of motion for the system. In the case of the time-averaging the motion of the system is at all times 'constrained' by the integrals of motion, resulting in multi-periodic correlation functions that show no decay in time[33]. For the ensemble case, the averaged correlation function get contributions from many 'systems' which have different values of the integrals of motion that results in an effective cancellation of periodic oscillations, leading to a decay of the correlation functions.

The behavior of the correlation functions for the single system may be broadly explained in this way: The oscillations of the correlation function reflect that the system is in some sense close to being exactly solvable. These features will probably vanish if further terms are included into the Hamiltonian in Eq. (2). The most natural term would be the dipole-dipole interaction between the nuclei which would kill most of the integrals of motion. It is important to recognize that the timescale related to the dipole-dipole interaction is very long, of the order 10^{-3} s, and the resulting decay time would reflect that.

In connection to coherently controlling the spin, the motion of the electron spin in the effective nuclear magnetic field will cause 'errors'. Even though in this model nuclear spins do not decohere the electron spin (in the sense of not causing decay of correlation functions as a function of time), they leads to a complicated, and unpredictable, evolution. Consequently, an electron spin initially in $|\uparrow\rangle$ can be found in the opposite spin state on a timescale $\propto \gamma^{-1}$. Thus, even though the hyperfine coupling to the nuclear system does not lead to decoherence in this model it can strongly affect the dynamics of the electron spin.

The authors acknowledge financial support from FOM and SIE would like to thank Oleg Jouravlev, Dmitri Bagrets and Lieven Vandersypen for fruitful discussions.

APPENDIX A: THE VARIANCE IN TERMS OF g_b

The initial condition for each nuclear spin subsystem is chosen from a Gaussian distribution whose variance is determined by

$$\langle \boldsymbol{K}_b^2 \rangle \;=\; \gamma^2 I(I+1) g_b^2 C_n V_b. \tag{A1}$$

where V_b is the volume of subsystem b, and $C_n V_b$ is the associated number of nuclear spins in that volume. For the calculations it is convenient to express the variance for a given subsystem only in terms of the coupling g_b by expressing the subsystem volume V_b as a function of g_b. The volume of the subsystem V_b is related to g_b via

$$V_b \;\equiv\; \left|\frac{dV}{dg}\right|_{g=g_b} \delta g, \tag{A2}$$

where V is the volume of the region where $g \geq g_b$. The functional form of $g(\boldsymbol{r})$ is determined by the density $|\psi(\boldsymbol{r})|^2$. In the numerical calculations a lateral parabolic confinement of an underlying 2DEG is used. Assuming a constant electron density in the z direction (growth direction) the electron density is

$$g(\boldsymbol{r}) = \theta(z_0/2 - |z|)\exp(-(x^2+y^2)/\ell^2), \tag{A3}$$

which gives the simple relation $x^2 + y^2 = \ell^2 \ln(1/g)$, within the 2DEG. Using the relation for the volume $V(\boldsymbol{r}) = z_0\pi(x^2+y^2)$ the subsystem volume is

$$V_b \;=\; V_{\rm QD}\frac{\delta g}{g_b}, \tag{A4}$$

which gives the variance of the distribution of the effective nuclear magnetic field for a given subsystem in terms of the coupling

$$\langle \boldsymbol{K}_b^2 \rangle \;=\; \gamma^2 N I(I+1) g_b \delta g. \tag{A5}$$

These results can be used to calculate the variance of the total nuclear spin defined in Eq. (30)

$$\langle \boldsymbol{I}^2 \rangle \;=\; \sum_{b,b'} \frac{\langle \boldsymbol{K}_b \cdot \boldsymbol{K}_{b'} \rangle}{g_b g_{b'}} \tag{A6}$$

$$\;=\; \frac{\langle \boldsymbol{K} \rangle}{\overline{g^2}} \sum_b \frac{\delta g}{g_b} \tag{A7}$$

$$\;\approx\; \frac{\langle \boldsymbol{K} \rangle}{\overline{g^2}} \ln(2N_b), \quad N_b \gg 1. \tag{A8}$$

In the last step it is assumed that $g_b = 1 - (b-1/2)/N_b$, resulting in the logarithm.

* Present address: Department of Physics and Astronomy, University of Basel, Klingelbergstrasse 82, CH-4056, Switzerland

[1] D. D. Awshalom, D. Loss, and N. Samarth, eds., *Semiconductor Spintronics and Quantum Computation* (Springer-Verlag, Berlin, 2002).
[2] A. Steane, Rep. Prog. Phys. **61**, 117 (1998).
[3] A. Shnirman, G. Schön, and Z. Hermon, Phys. Rev. Lett. **79**, 2371 (1997).
[4] D. Loss and D. P. DiVincenzo, Phys. Rev. A **57**, 120 (1998).
[5] B. E. Kane, Nature **393**, 133 (1998).
[6] Y. Nakamura, Y. A. Pashkin, and J. S. Tsai, Nature **398**, 786 (1999).
[7] J. E. Mooij, T. P. Orlando, L. Levitov, L. Tian, and C. H. van der Wal, Science **285**, 1036 (1999).
[8] L. M. K. Vandersypen, M. Steffen, G. Breyta, C. S. Yannoni, M. H. Sherwood, and I. L. Chuang, Nature **414**, 883 (2001).
[9] A. V. Khaetskii and Y. V. Nazarov, Phys. Rev. B **61**, 12639 (2000).
[10] A. V. Khaetskii and Y. V. Nazarov, Phys. Rev. B **64**, 125316 (2001).
[11] S. I. Erlingsson, Y. V. Nazarov, and V. I. Fal'ko, Phys. Rev. B **64**, 195306 (2001).
[12] S. I. Erlingsson and Y. V. Nazarov, Phys. Rev. B **66**, 155327 (2002).
[13] L. M. Woods, T. L. Reinecke, and Y. Lyanda-Geller, Phys. Rev. B **66**, 161318(R) (2002).
[14] Y. B. Lyanda-Geller, I. L. Aleiner, and B. L. Altshuler, Phys. Rev. Lett. **89**, 107602 (2002).
[15] T. Fujisawa, Y. Tokura, and Y. Hirayama, Phys. Rev. B **63**, R81304 (2001).
[16] T. Fujisawa, D. G. Austing, Y. Tokura, Y. Hirayama, and S. Tarucha, Nature **419**, 278 (2002).
[17] R. Hanson, B. Witkamp, L. M. K. Vandersypen, L. H. Willem van Beveren, J. M. Elzerman, and L. P. Kouwenhoven, Phys. Rev. Lett. **91**, 196802 (2003).
[18] A. V. Khaetskii, D. Loss, and L. Glazman, Phys. Rev. Lett. **88**, 186802 (2002).
[19] J. Schliemann, A. V. Khaetskii, and D. Loss, Phys. Rev. B **66**, 245303 (2002).
[20] I. A. Merkulov, A. L. Efros, and M. Rosen, Phys. Rev. B **65**, 205309 (2002).
[21] Y. G. Semenov and K. W. Kim, Phys. Rev. B **67**, 73301 (2003).
[22] R. de Sousa and S. Das Sarma, Phys. Rev. B **67**, 033301 (2003).
[23] R. de Sousa and S. Das Sarma, Phys. Rev. B **68**, 115322 (2003).
[24] M. I. D'yakonov and V. Y. Kachorovksii, Sov. Phys. Semicond. **20**, 110 (1986).
[25] A. Khaetskii, D. Loss, and L. Glazman, Phys. Rev. B **67**, 195329 (2003).
[26] S. W. Brown, T. A. Kennedy, and D. Gammon, Solid State Nucl. Magn. Reson. **11**, 49 (1998).
[27] S. Tarucha, D. G. Austing, T. Honda, R. J. van der Hage, and L. P. Kouwenhoven, Phys. Rev. Lett. **77**, 3613 (1996).
[28] J. M. Elzerman, R. Hanson, J. S. Greidanus, L. H. Willem van Beveren, S. Di Franceschi, L. M. K. Vandersypen, S. Tarucha, and L. P. Kouwenhoven, Phys. Rev. B **67**, 161308 (2003).
[29] D. Paget, G. Lampel, B. Sapoval, and V. I. Safarov, Phys. Rev. B **15**, 5780 (1977).
[30] M. Dobers, K. v. Klitzing, J. Schneider, G. Weimann, and K. Ploog, Phys. Rev. Lett. **61**, 1650 (1988).
[31] L. I. Schiff, *Quantum Mechanics* (McGraw-Hill Book Company, New York, 1968), 3rd ed.
[32] A. M. O. deAlmeida, *Hamiltonian systems: chaos and quantization* (Cambridge University Press, Cambridge, 1988).
[33] J. Schliemann, private communication.

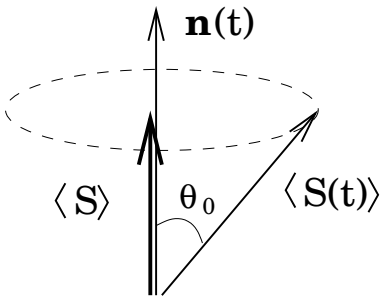

FIG. 1: The time dependent electron spin $\langle \boldsymbol{S}(t) \rangle$ precesses rapidly around the total effective magnetic field, resulting in a slowly varying average spin $\langle \boldsymbol{S} \rangle$ that the nuclei see. The angle between the instantaneous electron spin and $\boldsymbol{n}$ is θ_0

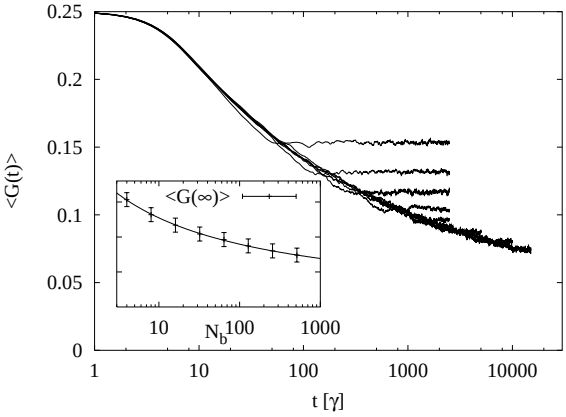

FIG. 2: The ensemble averaged correlation function as a function of time for $N_b = 4, 8, 16, 32, 64, 128, 256$ and 512. The inset show the asymptotic values of $\langle G(t) \rangle$ and a fit to $\alpha / \ln(\beta N_b)$.

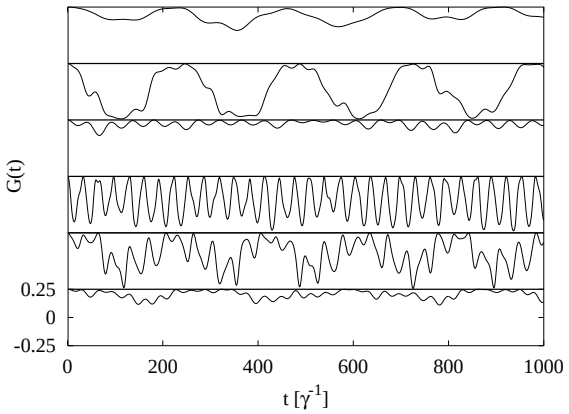

FIG. 3: Numerical calculations of the correlation function $G(t)$ for $N_b = 8$ and various randomly chose initial conditions. The curves are offset for clarity and the vertical range is the same for all curves, i.e. -0.25 to 0.25

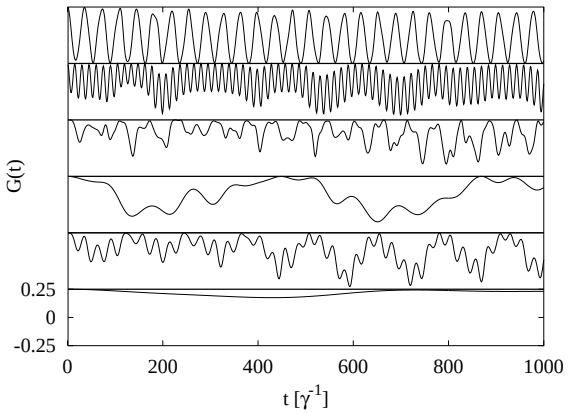

FIG. 4: Numerical calculations of the correlation function $G(t)$ for $N_b = 32$ and various randomly chose initial conditions. The curves are offset for clarity and the vertical range is the same for all curves, i.e. -0.25 to 0.25

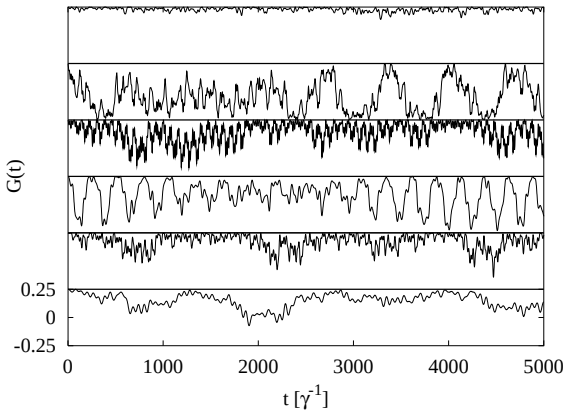

FIG. 5: Numerical calculations of the correlation function $G(t)$ for $N_b = 128$ and various randomly chose initial conditions. The curves are offset for clarity and the vertical range is the same for all curves, i.e. -0.25 to 0.25

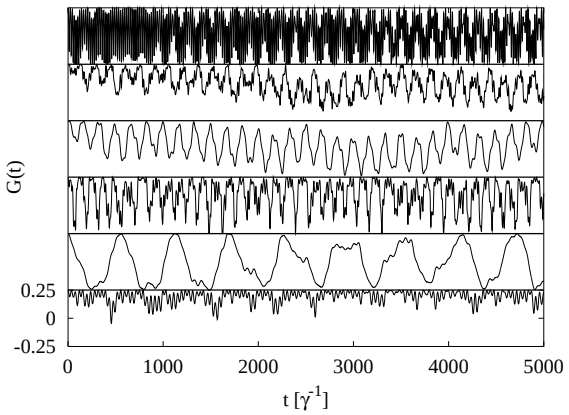

FIG. 6: Numerical calculations of the correlation function $G(t)$ for $N_b = 256$ and various randomly chose initial conditions. The curves are offset for clarity and the vertical range is the same for all curves, i.e. -0.25 to 0.25

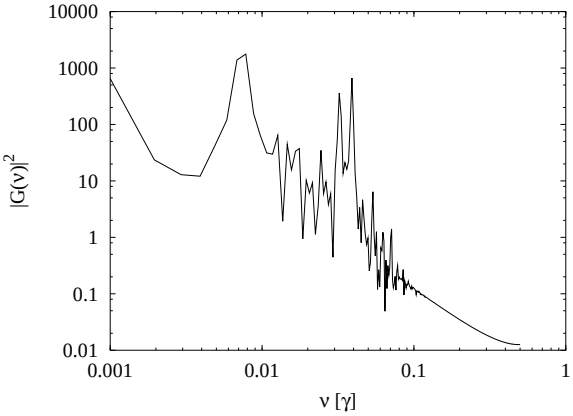

FIG. 7: The power spectrum of the 2nd curve (counted from the bottom one) in Fig. 4, corresponding to $N_b = 32$.

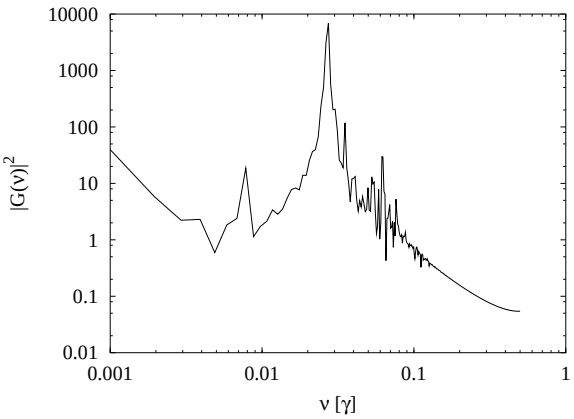

FIG. 8: The power spectrum of the 6th curve (counted from the bottom one) in Fig. 4, corresponding to $N_b = 32$.

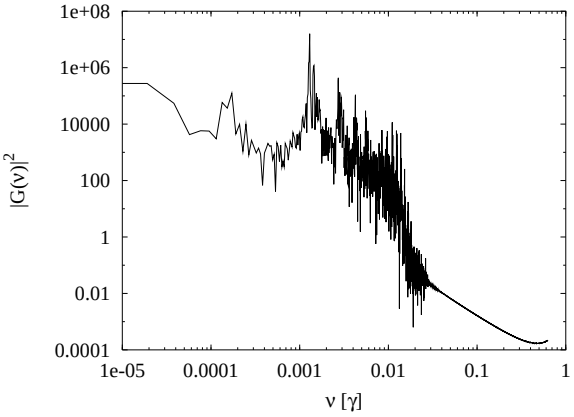

FIG. 9: The power spectrum of the 2nd curve (counted from the bottom one) in Fig. 6, corresponding to $N_b = 256$.

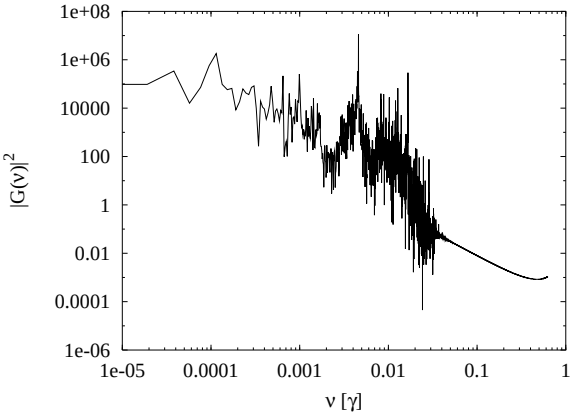

FIG. 10: The power spectrum of the fourth lowest curve in Fig. 6, corresponding to $N_b = 256$

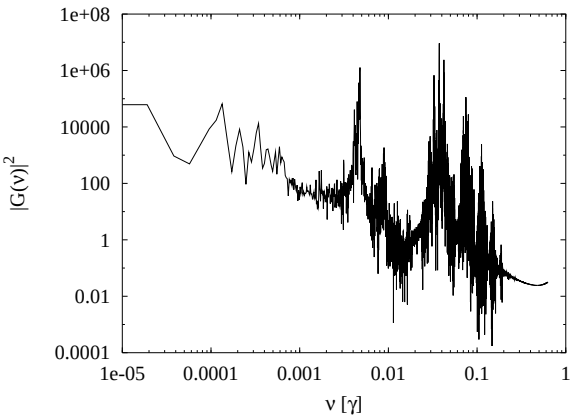

FIG. 11: The power spectrum of the top curve in Fig. 6, corresponding to $N_b = 256$